2nd Conference for Engineering Sciences
and Technology -CEST2 29-31 October 2019
- Sabratha –Libya

Real Implementation of Advanced Strategies for Vector Control of Induction Motors

El-Sharif A. Omer[1], Mohamed M. Ali [2], Mohammed A. Elmadi[3]

[1] sharifabdomar@hotmail.com, [2] shaglouf@su.edu.ly, [3]Eng.abusaleem84@gmail.com

[1,2,3] Electrical Engineering Department, Faculty of Engineering, Sirte University, Libya

ABSTRACT

This paper documents the work carried out to investigate and analyze a number of open problems in speed control of induction motors. The work involves theoretical and simulation studies, as well as hardware design, implementation and experimental results. The hardware is based on Digital Signal Processing (DSP) technology which allows flexible implementation of advanced control strategies in real-time. Various aspects of induction motor control were studied, including simulations of vector control, speed sensorless control, advanced input-output decoupling and nonlinear flux observers. In addition, a number of algorithms were implemented and experimentally evaluated on the hardware rig, designed as part of the paper. These include Field Oriented Control and speed-sensorless vector control. A number of relevant conclusions connected with induction motor control are presented.

Keywords: Induction Motors, Vector Control, Field Oriented Control.

1 Introduction

Although induction motors have a very simple structure, high efficiency, economical advantages, less cost, and small size and reliability, their mathematical model is complex due to the coupling factor between a large number of variables and the non-linearities. This makes its application at variable speed more complex than DC machines. The rapid developments in the field of power electronics and the existence of powerful and inexpensive microprocessors, which allow complex control functions to be implemented in software rather than on expensive hardware, and the development and implementation of vector control techniques [1, 2, 3] have made AC drives compete with DC in high performance applications. Open loop control methods, such as a standard v/f control, may provide a satisfactory variable speed drive when the motor has to operate at steady torque without stringent requirements on speed regulation. However, when fast dynamic response and accurate speed regulation are required, open loop control is unsatisfactory [4, 5].

A control technique introduced by Blaschke [5], called vector control that is based on a complete dynamic state-space model of the motor yields better dynamics for torque variations along a wider speed range. The vector control scheme consists of controlling the stator currents represented by a space vector [2]. This technique is based on projections, which transform a three-phase time system into a two coordinate (d and q coordinates) time invariant system. These projections lead to a model structure that is similar to that of a DC machine. By regulating the amplitude of the rotor flux, a linear relationship between torque and the projected torque-producing current component (isq) is obtained. Consequently, it is straightforward to control the torque by controlling the

torque component of the stator current vector [2, 5, 6].
The vector control technique enables to operate the drive beyond the nominal speed (field-weakening) approach. This could be achieved by adjusting the reference for the rotor flux to keep the stator voltages from saturating at high speed.
The drawback of the classical vector control technique is that the method assumes that the magnitude of the rotor flux is constantly regulated to a fixed value, which is not the case during the flux transient. Therefore, the speed is not completely decoupled from the rotor flux. This technique was therefore improved by achieving exact input-output decoupling and linearization via a nonlinear state feedback control [6, 7]. A similar technique was used to achieve a sliding mode controller for input-output decoupling of rotor flux and speed. The drawback of the input-output decoupling algorithm is the need of flux sensors, which are to be inserted in the air-gap. This reduces the reliability and implies both additional costs and technological difficulties [8]. Therefore, on the basis of the rotor speed ω_r, stator currents (i_{sa}, i_{sb}) and stator voltages (V_{sa}, V_{sb}), flux observers have been developed [9]. Uncertainties of crucial parameters of the machine such as the rotor resistance and load torque that affect the accuracy in the field oriented control and input-output decoupling algorithms were studied in [6, 7, 8, 10].
Throughout the last decade, there has been much research that aimed to high-performance sensorless control of position or speed in induction motors. Some are based on non-linear observer structure and Kalman estimators [7] and some are based on Model Reference Adaptive Control (MRAC) [2]. Both approaches are poor at low and zero speed due to machine parameters dependency. The problem of flux and speed estimation at low speed is the single biggest problem in induction motor drive research [11]. Attempts to solve this problem by estimating the flux position which is independent of motor parameters by using high frequency signal injection and slot harmonics techniques are found in [1, 2, 3, 10].
More recent developments in induction motor control make use of intelligent control techniques such as neural networks and fuzzy logic to handle higher levels of uncertainty that might consist of whole functions and not just parameters [5, 8]. This project will focus on the theoretical investigations and simulation of a number of strategies for vector controlled induction motor drives.

2 Theory of Induction Motor and Modeling

2.1 Transformations between Frames

In order to transform any two-phase vectors from a frame y to another frame x or vice-versa, the following transformations are used:

$$\begin{bmatrix} x_1 \\ x_2 \end{bmatrix} = \begin{bmatrix} \cos\theta & -\sin\theta \\ \sin\theta & \cos\theta \end{bmatrix} \begin{bmatrix} y_1 \\ y_2 \end{bmatrix} \quad (1)$$

$$\begin{bmatrix} y_1 \\ y_2 \end{bmatrix} = \begin{bmatrix} \cos\theta & \sin\theta \\ -\sin\theta & \cos\theta \end{bmatrix} \begin{bmatrix} x_1 \\ x_2 \end{bmatrix} \quad (2)$$

Where y1, y2 are the components of the vector to be transformed and θ is the instantaneous angle from the y frame to the x frame.
In order to transform three-phase components (A,B,C) to two-phase components expressed in the (a,b) stationary reference frame and vice-versa, the following transformations are required:

$$\begin{bmatrix} X_0 \\ X_a \\ X_b \end{bmatrix} = \frac{2}{3}\begin{bmatrix} 1/2 & 1/2 & 1/2 \\ 1 & -1/2 & -1/2 \\ 0 & \sqrt{3}/2 & -\sqrt{3}/2 \end{bmatrix}\begin{bmatrix} X_A \\ X_B \\ X_C \end{bmatrix} \quad (3)$$

$$\begin{bmatrix} X_A \\ X_B \\ X_C \end{bmatrix} = \frac{3}{2}\begin{bmatrix} 2/3 & 2/3 & 0 \\ 2/3 & -1/3 & 1/\sqrt{3} \\ 2/3 & -1/3 & -1/\sqrt{3} \end{bmatrix}\begin{bmatrix} X_0 \\ X_a \\ X_b \end{bmatrix} \quad (4)$$

where X0 is the zero sequence component. When the above transformations are used, the peak two-phase quantities are equal to the peak three-phase quantities.

2.2 Single Cage Induction Machine Model in the (d,q) Synchronous Reference Frame

The three phase stator voltage equations of a single cage induction motor expressed in the stator reference frame are:

$$\underline{V}_{s\,A,B,C} = R_s \underline{i}_{s\,A,B,C} + \frac{d\underline{\Psi}_{s\,A,B,C}}{dt} \quad (5)$$

Using Equation (3) the stator voltage equations can be transformed from three phase quantities into two phase ones and the following two equations are obtained. A detailed analysis for transforming the three phase system to two phase system can be found in [2, 3].

$$V_{sa} = R_s i_{sa} + \frac{d\Psi_{sa}}{dt} \quad (6)$$

$$V_{sb} = R_s i_{sb} + \frac{d\Psi_{sb}}{dt} \quad (7)$$

Similarly, the three phase rotor voltages equations of a single cage induction motor expressed in the rotor reference frame are:

$$\underline{V}_{r\,A,B,C} = R_r \underline{i}_{r\,A,B,C} + \frac{d\underline{\Psi}_{r\,A,B,C}}{dt} \quad (8)$$

Using Equation (3) the rotor voltage equations can be transformed from three phase quantities into two phase ones and the following two equations are obtained:

$$0 = R_r i_{r\alpha} + \frac{d\Psi_{r\alpha}}{dt} \quad (9)$$

$$0 = R_r i_{r\beta} + \frac{d\Psi_{r\beta}}{dt} \quad (10)$$

The study of the induction machine in the synchronous reference frame is very important since the necessary equations of vector control theory are based on this model and the controller requires the feedback information in the synchronous frame. The idea of a revolving the (d,q) synchronous reference frame is introduced [9] to transform the ac components of vectors in the stator frame into dc signals as it will be seen in the next section. This frame rotates at angular frequency ωe which satisfies the following Equation (11), where θe is the angle between the d-axis of the rotor flux frame and the a-axis of the stator frame.

$$\omega_e = \frac{d\theta_e}{dt} \quad (11)$$

The stator and rotor voltage Equations (6), (7) and (9), (10) have been given in their natural reference frames. By utilizing the transformation given in Equation (2), the single cage induction machine model in the (d,q) rotor flux frame is obtained [1]:

$$\underline{V}_{sd,q} = R_s \underline{i}_{s\,d,q} + \frac{d\underline{\Psi}_{s\,d,q}}{dt} + j\omega_m \underline{\Psi}_{s\,d,q} \tag{12}$$

$$0 = R_r \underline{i}_{r\,d,q} + \frac{d\underline{\Psi}_{r\,d,q}}{dt} + j(\omega_m - \omega_r)\underline{\Psi}_{r\,d,q} \tag{13}$$

Since the states have been chosen as the rotor fluxes (Ψrd , Ψrq) and the stator currents (isd , isq), Equations (12) and (13) expressed in the synchronous frame are used to express the stator fluxes (Ψsd , Ψsq) and the rotor currents (ird , irq) in terms of the rotor fluxes and the stator currents. Consequently the following dynamic model of induction machine in the (d,q) synchronous frame is obtained:

$$\begin{aligned}
\frac{d\omega_r}{dt} &= \mu\left(\Psi_{rd} i_{sq} - \Psi_{rq} i_{sd}\right) - \frac{T_L}{J} \\
\frac{d\Psi_{rd}}{dt} &= -\alpha\Psi_{rd} + \alpha L_m i_{sd} + \omega_{sl}\Psi_{rq} \\
\frac{d\Psi_{rq}}{dt} &= -\alpha\Psi_{rq} + \alpha L_m i_{sq} - \omega_{sl}\Psi_{rd} \\
\frac{di_{sd}}{dt} &= -\gamma i_{sd} + \alpha\beta\Psi_{rd} + \omega_e i_{sq} + \beta\omega_r\Psi_{rq} + \frac{1}{\sigma L_s} V_{sd} \\
\frac{di_{sq}}{dt} &= -\gamma i_{sq} + \alpha\beta\Psi_{rq} - \omega_e i_{sd} - \beta\omega_r\Psi_{rd} + \frac{1}{\sigma L_s} V_{sq} \\
T &= P\frac{L_m}{L_r}\left(\Psi_{rd} i_{sq} - \Psi_{rq} i_{sd}\right)
\end{aligned} \tag{14}$$

Where:

$\sigma = 1 - \frac{L_m^2}{L_s L_r}$, $\alpha = \frac{R_{rN}}{L_r}$, $\beta = \frac{L_m}{\sigma L_s L_r}$, $\gamma = \frac{L_m^2 R_{rN}}{\sigma L_s L_r^2} + \frac{R_s}{\sigma L_s}$, $\mu = \frac{P L_m}{j L_r}$ and P is pole pairs.

3 Induction Motor Control

Although the induction machine is superior to the DC machine with respect to many factors such as size, rotor inertia, reliability and maximum speed, it entails more complex control schemes than the excited DC machine, because of its highly coupled and nonlinear dynamic structure. However, the existence of vector control and the rapid developments in microprocessors have made AC drives competitive with high performance four quadrant DC machines. Therefore, in this paper, much attention is paid to the vector control algorithm.

3.1 v/f Drive

The speed and the torque of an induction machine can be controlled by varying the stator voltage Vs and the supply frequency ωs in proportion to each other. This has the effect of maintaining the stator flux constant. Such a scheme is called a Constant Volts per Hertz (v/f) drive. The practical implementation of a v/f drive is based on the steady-state model of the induction motor. This makes the scheme poor during the flux

transient operation.

3.2 Vector Control of Induction Motor

The vector control scheme enables the control of the induction motor in the same way as a separately excited DC motor. As in the DC motor, torque control of the induction motor is achieved by controlling the torque current component (q-axis component) and flux control is achieved by controlling the flux current component (d-axis component) independently. The advantage of the vector control technique over the v/f drive is that, the latter is based on the steady-state equivalent circuit of the induction motor and therefore unsuitable for high performance applications, while the former is based on the full dynamic equivalent circuit of the induction motor and therefore responds more efficiently to the highly dynamic environment of variable speed applications. It is concluded in [2], that the behaviour of stator flux is very similar to air gap flux orientation. On the other hand from a comparison between stator flux orientation and rotor flux orientation [2], it was concluded that the latter is preferred due to the absence of cross coupling terms between the flux and torque producing current. An implementation of stator flux orientation can be found in [8].

3.2.1 Rotor Flux Orientation

By aligning the rotor flux with the real axis of the synchronous frame, Ψrq equals zero and θm equals θe. Substituting these values in the induction motor model in the (d,q) frame Equation (14), the following closed loop model is obtained

$$\frac{d\omega_r}{dt} = \mu \Psi_{rd} i_{sq} - \frac{T_L}{J} \tag{15}$$

$$\frac{d\Psi_{rd}}{dt} = -\alpha \Psi_{rd} + \alpha L_m i_{sd} \tag{16}$$

$$0 = \alpha L_m i_{sq} - \omega_{sl} \Psi_{rd} \tag{17}$$

$$\frac{di_{sd}}{dt} = -\gamma i_{sd} + \alpha\beta \Psi_{rd} + \omega_m i_{sq} + \frac{1}{\sigma L_s} V_{sd} \tag{18}$$

$$\frac{di_{sq}}{dt} = -\gamma i_{sq} - \omega_m i_{sd} - \beta \omega_r \Psi_{rd} + \frac{1}{\sigma L_s} V_{sq} \tag{19}$$

$$T = P \frac{L_m}{L_r} \Psi_{rd} i_{sq} \tag{20}$$

It follows from Equation (20) that when flux Ψrd is regulated, the torque T is proportional to isq which is similar to the torque equation of the separately excited DC motor. Equation (16) provides a means of regulating the rotor flux linkage Ψrd by controlling isd. On the other hand, with Ψrd regulated, isq can control the torque directly as in Equation (20). The slip speed can be obtained from Equation (17) by applying Indirect Rotor Field Orientation (IRFO) [12] or Direct Rotor Field Orientation (DRFO) techniques to estimate the angle θm.

3.3 Adaptive Control of Induction Motor

This section looks at parameter adaptive control of the induction motor. A rotor speed estimator which utilizes only the stator current as feedback information to the DSP is discussed and simulated. In addition to that, uncertain parameters of induction motor such as rotor resistance Rr and load Torque TL are considered by simulating estimators

which attempts to capture these uncertainties. The reader is referred to [13] and [14] for the general theory of adaptive control.

3.3.1 Model Reference Adaptive Control (MRAC)

Model reference adaptive control systems are a special type of adaptive systems. It possesses attractive features that lead to relatively simple implementations. The MRAC need not be implemented in actual hardware. It can be a mathematical algorithm implemented on a computer. In such systems, the error between the outputs of the reference model and the adjustable model is used by an adaptation mechanism either to modify the parameters of the adjustable model or to generate the control signals which force the output error between the reference model and the adjustable model to converge to zero. There are various types of MRAC [15].

3.3.2 Rotor Speed Estimator

In this estimator [16], the MRAC uses the rotor magnetizing current imr vector (rotor flux linkage vector) as error to estimate the rotor frequency ωr. The rotor magnetising current expressed in the (d,q) reference frame is defined as:

$$\mathbf{i}_{\mathbf{mr}(d,q)} = \frac{\mathbf{\Psi}_{\mathbf{r}(d,q)}}{L_m} \tag{21}$$

The relationship of the modified rotor magnetizing current vector $\mathbf{i'_{mr}}$ and the rotor magnetizing current vector imr is:

$$\frac{d\mathbf{i}_{\mathbf{mr}(d,q)}}{dt} + j\omega_m \mathbf{i}_{\mathbf{mr}(d,q)} = \frac{d\mathbf{i}'_{\mathbf{mr}(d,q)}}{dt} + \frac{\mathbf{i}'_{\mathbf{mr}(d,q)}}{T_1} + j\omega_m \mathbf{i}'_{\mathbf{mr}(d,q)} \tag{22}$$

By utilizing Equation (21) and the stator voltage of Equation (12) and Equation (22), the following differential equations are obtained for the modified rotor magnetizing current expressed in the (d,q) frame.

$$\frac{di'_{md}}{dt} + \frac{i'_{md}}{T_1} - \omega_m i'_{mq} = \frac{L_r}{L_m^2}\left(V_{sd} - R_s i_{sd} - \sigma L_s \frac{di_{sd}}{dt} + \sigma L_s \omega_m i_{sq}\right) \tag{23}$$

$$\frac{di'_{mq}}{dt} + \frac{i'_{mq}}{T_1} + \omega_m i'_{md} = \frac{L_r}{L_m^2}\left(V_{sq} - R_s i_{sq} - \sigma L_s \frac{di_{sq}}{dt} - \sigma L_s \omega_m i_{sd}\right) \tag{24}$$

where i'_{md} and i'_{mq} are the d and q components of the modified rotor magnetizing current vector, V_{sd} and V_{sq} are the d and q components of the stator voltage vector, i_{sd} and i_{sq} are the d and q components of the stator current, Tr is the rotor time constant, Rr is the stator resistance, Lr is the rotor inductance, Ls is the stator inductance, Lm is the magnetizing inductance of the machine, ωm is the rotor magnetizing current frequency.

By substituting Equation (21) into the rotor voltage of Equation (13) , the following differential equation is obtained for the rotor magnetizing current expressed in the (d,q) frame.

$$\frac{d\mathbf{i}_{mr(d,q)}}{dt} = \frac{\mathbf{i}_{s(d,q)}}{T_r} - \mathbf{i}_{mr(d,q)}\left(\frac{1}{T_r} + j(\omega_m - \omega_r)\right)$$

(25)

By considering Equation (22) , Equation (25) can be expressed in terms of the modified rotor magnetizing current as:

$$\frac{d\mathbf{i}'_{mr(d,q)}}{dt} = \frac{\mathbf{i}_{s(d,q)}}{T_r} - \mathbf{i}'_{mr(d,q)}\left(\frac{1}{T_1} + j\omega_m\right) - \mathbf{i}_{mr(d,q)}\left(\frac{1}{T_r} - j\omega_r\right)$$

(26)

There are many ways to ensure the global stability of adaptive systems [2, 15]. By utilizing Equations (25) and (26), the identification algorithm for the rotor speed is obtained according to Popov's hyperstability criterion, which states that the linear time-invariant forward-path transfer function matrix must be strictly positive real and the non-linear time varying feedback has to satisfy Popov's integral inequality. This leads to the adaptive law [2]:

$$\hat{\omega}_r = \hat{\omega}_r(0) + k\hat{i}_{md}\int_0^t \left(\hat{\omega}_{sl}\left(i'_{md} - \hat{i}'_{md}\right) + \frac{d\left(i'_{mq} - \hat{i}'_{mq}\right)}{dt} + \frac{\left(i'_{mq} - \hat{i}'_{mq}\right)}{T_r}\right)dt \qquad (27)$$

where k > 0 , is the integral adaptation coefficient.

4 Results and Discussion

4.1 Simulation Results of Rotor Field Orientation

The performance of the rotor field oriented control is simulated according to the following sequence. The unloaded motor is required to reach the rated values for the speed and flux amplitude, i.e. a speed of 220 rad/sec and a flux of 1.3 web.
At t = 2 sec, a 40 Nm load torque is applied.
At t = 4 sec, the speed is required to reach 300 rad/sec (above the nominal speed), so the rotor flux reference is reduced according to the field weakening Equation Ψrdref=k/ωrref [5]. Four PI controllers are used in the full FOC implementation, two for isd and isq and two for Ψrd and ωr in cascade with the former pair.
The transfer function of the PI controllers used in this simulation is given by:

$$PI = \frac{ks + a}{s} \qquad (28)$$

The parameters k and a of the PI controllers have been tuned such that a compromise between minimum overshot and fast settling time is satisfied. Table 1 shows the values of the PI parameters used in the simulation and the corresponding damping ratio (ζ) and undamped natural frequency (ω).

Table 1: PI parameters used in simulations

PI	k	a	ζ	ω
Flux controller Ψrd	94.9	685.3	0.8	10
Current controller isd	4	8100	0.5	90
Current controller isq	4	8100	0.5	90
Speed controller ωr	16	100	0.8	10

The output responses of the rotor speed and the rotor flux are shown in Figure 1 and Figure 2 respectively, while Figure 3 shows the torque producing and flux producing currents isq and isd . It follows from these figures that the output responses track the reference signals. A small error occurs when the load torque is applied at t = 2 sec, but this error is immediately rectified by the PI controller.

The main drawback of this algorithm is that during the flux transient, the nonlinear term (Ψrd isq) in Equation (15), makes the algorithm nonlinear and coupled, because Ψrd is still not constant.

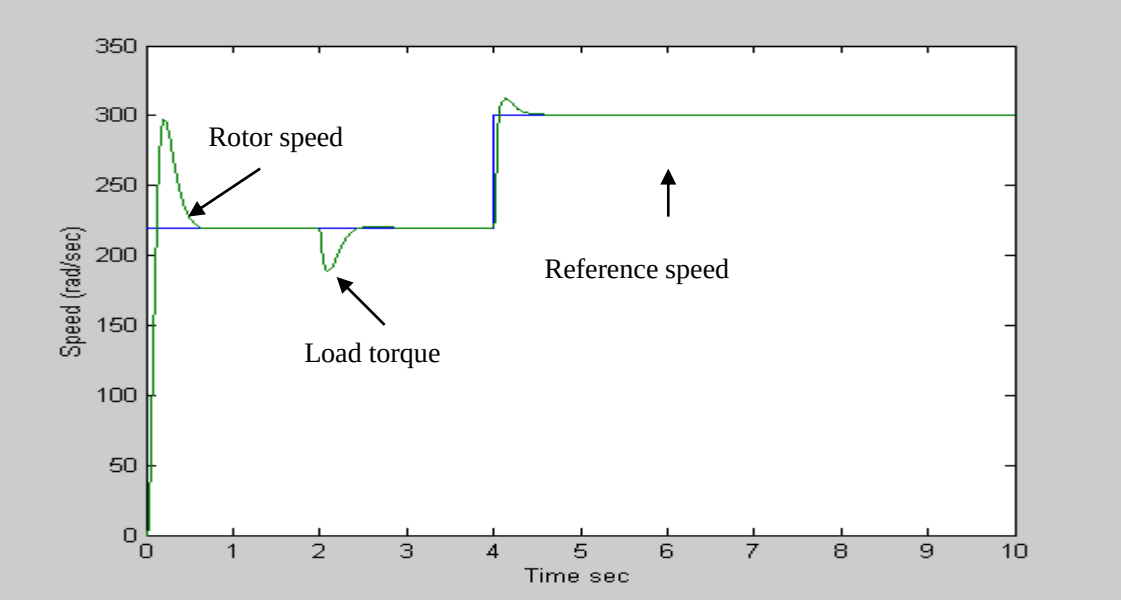

Figure 1: Rotor speed and load torque

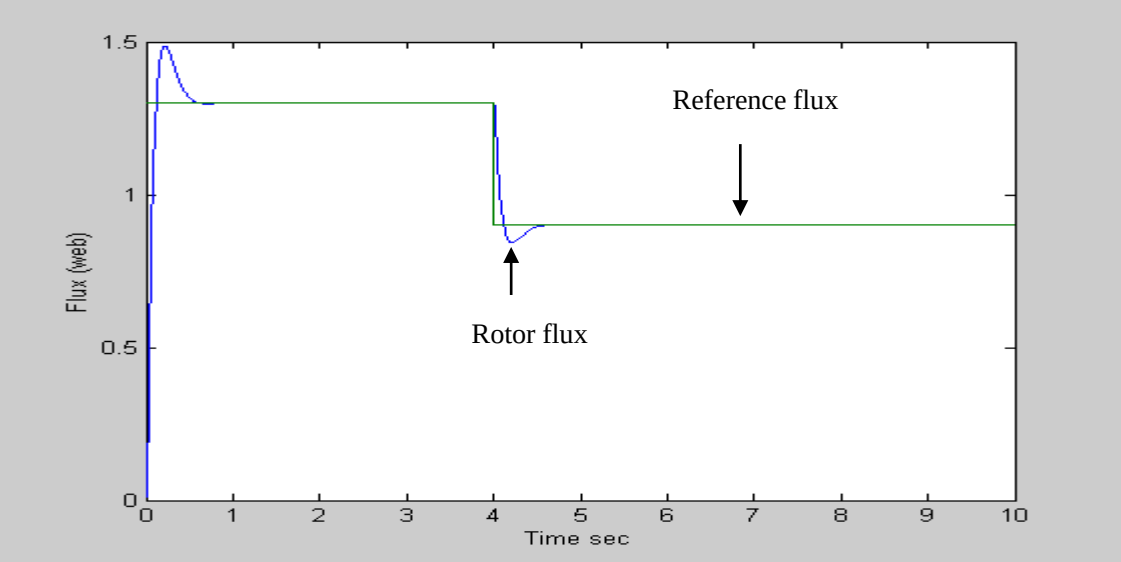

Figure 2: Rotor flux

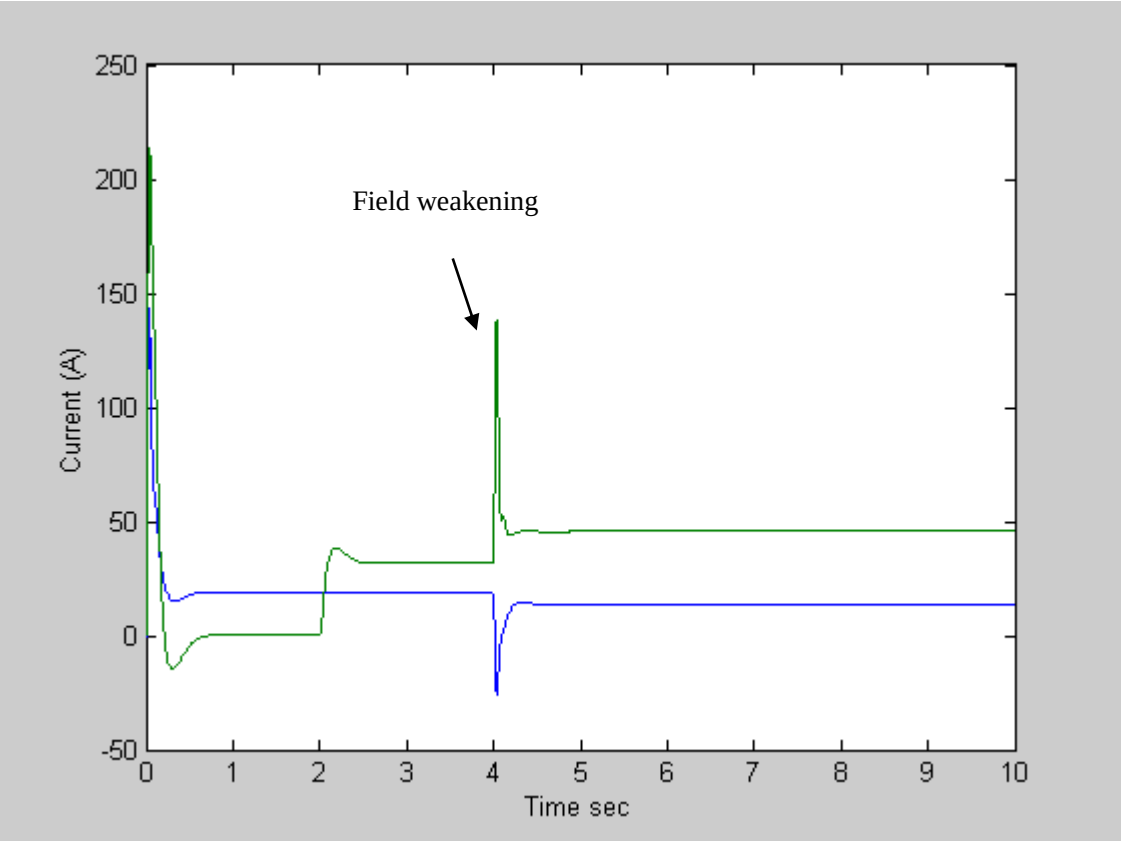

Figure 3: Torque i_{sq} and Flux i_{sd} producing currents

4.2 Simulation of the Rotor Speed Estimator

Figure 4 shows a satisfactory performance of this estimator even when the speed is in the field weakening region. As the time goes to infinity, the estimated and the actual speed are converging to each other. In the figure it is not possible to see the difference between the estimated and the actual speed because the curves are superimposed.

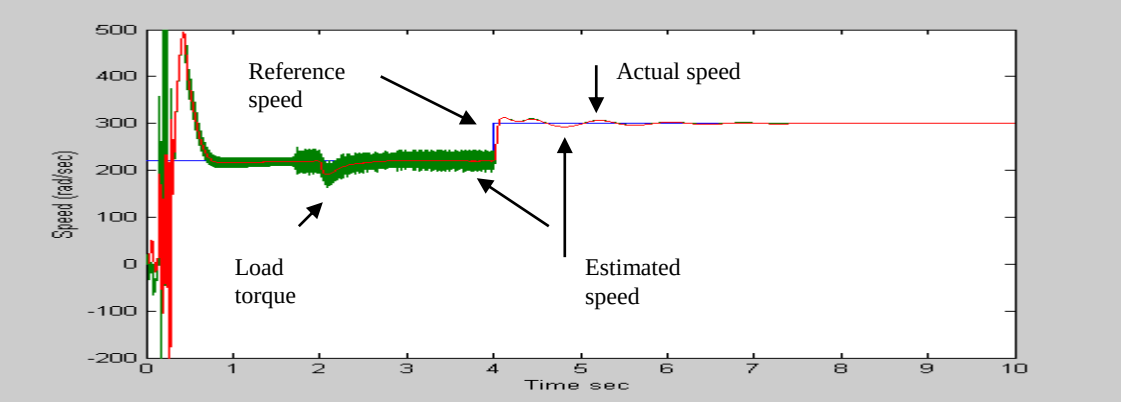

Figure 4: Estimated and actual rotor speed with field weakening

4.3 Experimental Results

4.3.1 Sensorless Speed Control Results

All the necessary equations required to implement the rotor speed estimator described in Section 3.3.2 were discretized at 200Hz sampling frequency and the standard vector control software was modified and developed accordingly. The sub-routine, which takes care of the rotor speed estimator, has been written in C language. The modified software was downloaded to the DSP and the hardware test rig was used. Figure 5 shows the performance of the rotor speed estimator when the motor was accelerated from rest to 900rpm. It follows from Figure 5 that, there is only slight difference between the actual and the estimated speed at low speed. It should be noted that the value of the adaptive gain k in Equation (27) was set to 20. Figures 6 and 7 shows the actual photos of the setup.

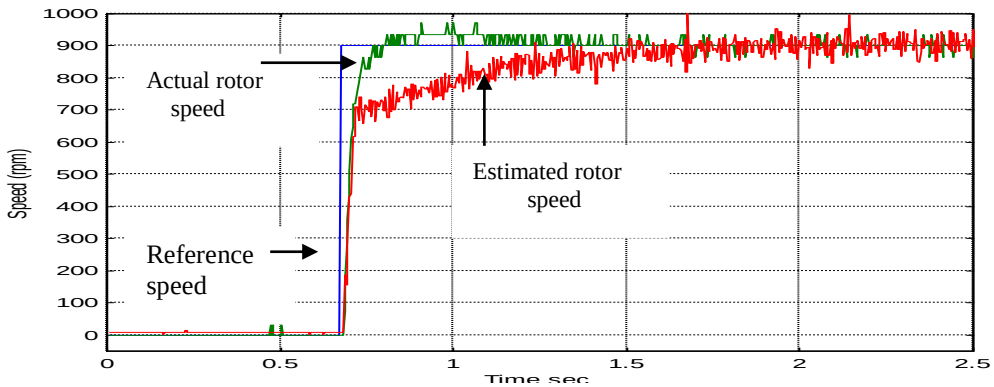

Figure 5: Actual and estimated speed when the reference speed changed (0 to 900rpm)

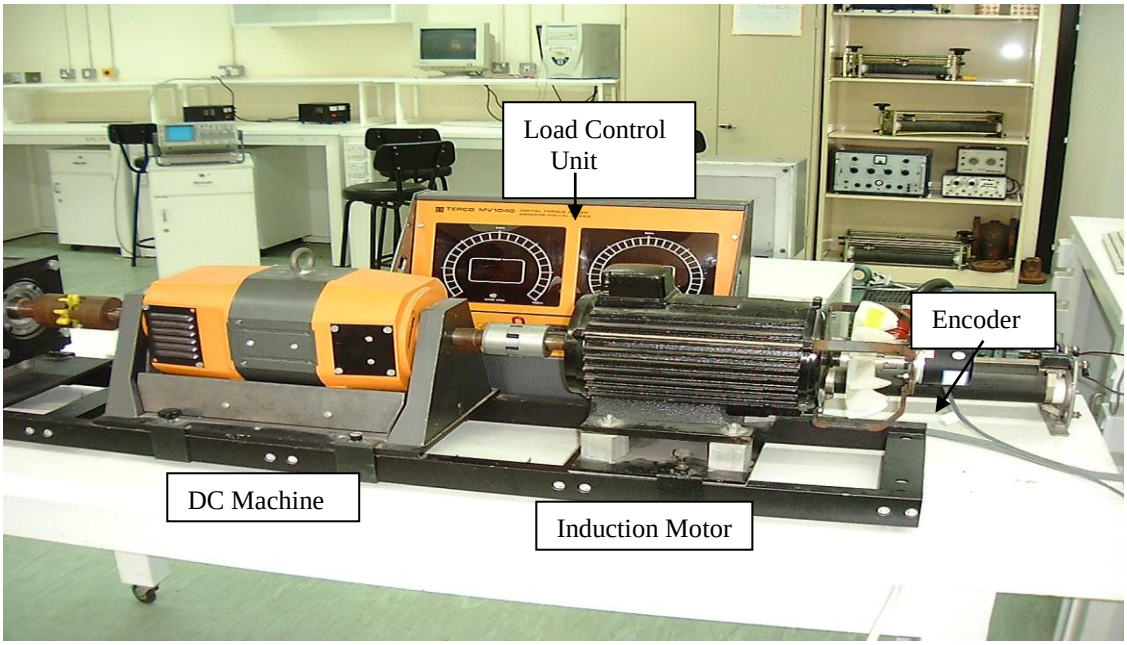

Figure 6: The induction motor and the DC machine for loading purposes

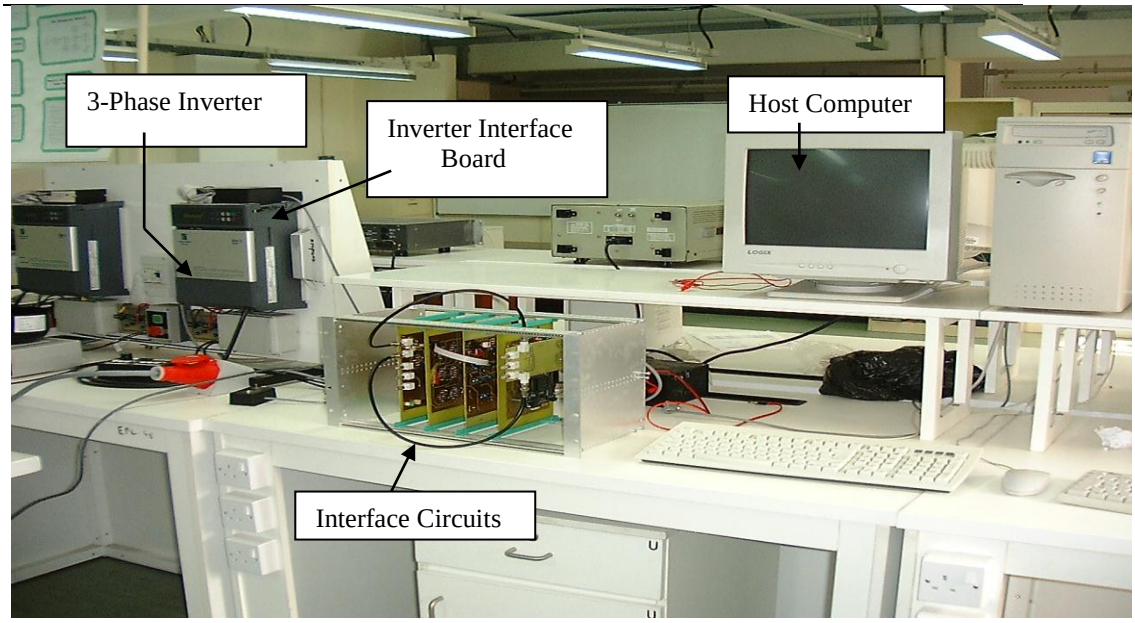

Figure 7: the experimental setup: the inverter interface circuit is housed inside the enclosure and situated on the top of the inverter, the host computer, DSP board and interface circuits.

5 Conclusions

The methodology of the paper was to first analyze and simulate the various control strategies to be investigated by using the Matlab/Simulink package. These strategies include vector control, nonlinear flux observers, in the case of classical control of induction motors, and sensorless speed vector controlled drives, rotor speed estimator and finally the adaptive version in the case of advanced control of induction motors.
Secondly, an experimental test rig that includes the fixed-point digital signal processor DSP unit was designed and set up, to implement some control strategies such as v/f drive, field oriented control and a sensorless speed vector controlled drive. Both the simulation and the practical results clearly show the improvement, fast performance and efficiency obtained by field oriented control. This technique makes the induction motor compete with the DC machine.

6 References

[1] J. Cilia, "Sensorless Speed and Position Control of Induction Motor Drives," PHD Thesis, University of Nottingham, 1997.

[2] P. Vas, Vector Control of AC Machines. Clarendon Press, Oxford, 1994.

[3] P. Vas, Electrical Machines and Drives. Clarendon Press, Oxford, 1992.

[4] SIMULINK a program for simulating dynamic systems: User's Guide, The Mathworks, Inc., Mass., USA, 2000.

[5] W. Leonhard, Control of Electrical Drives. Berlin: Springer-Verlag, 1985.

[6] R. Marino, S. Peresada, and P. Tomei, "Adaptive input-output linearizing control of induction motors," IEEE Trans. Automat. Contr., vol. 38, pp. 208-221, Feb 1993.

[7] R. Marino, S. Peresada, and P. Tomei, "Global adaptive output feedback control of induction motors with uncertain rotor resistance," IEEE Trans. Automat. Contr., vol. 44, pp. 967-983, May 1999.

[8] R. Marino, S. Peresada, and P. Tomei, “Output feedback control of current-feed induction motors with unknown rotor resistance,” IEEE Trans. on Control System Technology, vol. 4, pp. 336-346, July 1996.

[9] M. Trzynadlowski, Control of Induction Motors. Academic Press, USA, 2001.

[10] H. A. A. Fattah, and K. A. Loporo, “Speed control of electrical machines: unknown load torque case,” IEEE Trans. Automat. Contr., vol. 46, pp. 1979-1983, Dec. 2001.

[11] C. S. Staines, “Sensorless position estimation in asymmetric induction machines,” PhD Thesis, University of Nottingham, 1998.

[12] S. T. Nguyen, P. H. Pham, T. V. Pham, H. X. Ha, C. T. Nguyen, P. C. Do, "A sensorless three-phase induction motor drive using indirect field oriented control and artificial neural network", Industrial Electronics and Applications (ICIEA) 2017 12th IEEE Conference on, pp. 1454-1459, 2017.

[13] R. Isermann, K. Lachmann, and D. Matko, Adaptive Control System. Hertfordshire: Prentice-Hall, 1992.

[14] K. J. Astrom, and B. wittenmark, Adaptive Control. New York: Addison-Wesley, 1995.

[15] Y. Landau, Adaptive Control: The Model Reference Approach. Marcel Dekker Inc, 1979.

[16] D. Stojic, M. Milinkovic, S. Veinovic, I. Klasnic, "Improved Stator Flux Estimator for Speed Sensorless Induction Motor Drives", *Power Electronics*, vol. 30, no. 4, pp. 2363, April 2015.